J Appl Electrochem (2010) 40:409–417
DOI 10.1007/s10800-009-0011-3

ORIGINAL PAPER

Electrochemical impedance spectroscopy and cyclic voltammetry of ferrocene in acetonitrile/acetone system

Nikos G. Tsierkezos · Uwe Ritter

Received: 28 April 2009 / Accepted: 1 September 2009 / Published online: 19 September 2009

Abstract The oxidation of ferrocene ($FeCp_2$) to ferrocenium cation ($FeCp_2^+$) (where Cp: cyclopentadienyl anion, $C_5H_5^-$) was investigated by means of electrochemical impedance spectroscopy (EIS) and cyclic voltammetry (CV) on either platinum (Pt) or glassy carbon (G-C) electrodes in acetonitrile (ACN), acetone (ACE), and acetonitrile (ACN)/acetone (ACE) binary mixtures with *n*-tetrabutylammonium hexafluorophosphate ($TBAPF_6$) as background electrolyte at $T = 294.15$ K. The half-wave potentials ($E_{1/2}$), the diffusion coefficients (D), and the heterogeneous electron-transfer rate constants (k_s) were derived. The activation free energies for electron transfer ($\Delta G^{\neq}_{exp}$) were experimentally determined and compared with the theoretical values ($\Delta G^{\neq}_{cal}$). The electron-transfer process was reversible and diffusion-controlled in all investigated solvent mixtures. The changes on the metal–ligand bond lengths upon electron transfer were almost insignificant. The $E_{1/2}$ values were shifted to less positive potentials with the increase of the ACN content. The k_s values obtained on Pt electrode were slightly larger compared to k_s measured on G-C electrode, while in both cases the k_s values were diminished with the enrichment of the mixtures in ACN. The EIS spectra confirmed that the rate-determining step in the whole process is the diffusion of the $FeCp_2$ species and thus the process can be properly characterized as diffusion-controlled.

Keywords Activation free energy for electron transfer · Cyclic voltammetry · Diffusion coefficient · Electrochemical impedance spectroscopy · Ferrocene · Half-wave potential · Heterogeneous electron-transfer rate constant

N. G. Tsierkezos (✉) · U. Ritter
Institut für Physik, Fachgebiet Chemie, Fakultät für Mathematik und Naturwissenschaften, Technische Universität Ilmenau, Weimarer Straße 25, 98693 Ilmenau, Thüringen, Germany
e-mail: nikos.tsierkezos@tu-ilmenau.de

1 Introduction

The metallocenes (MCp_2) (where Cp: cyclopentadienyl anion) belong to the most important class of the organometallic compounds. MCp_2 are sandwich-type complexes in which the metal atom is sandwiched between the two Cp ligands [1]. The redox behavior of such sandwich complexes has been the subject of many investigations [2]. Ferrocene ($FeCp_2$), the first and prototypal member of metallocenes, exhibits a reversible one-electron oxidation process according to the reaction: $FeCp_2 \rightarrow FeCp_2^+ + e^-$. The oxidation of $FeCp_2$ to $FeCp_2^+$ has been proposed as standard one-electron transfer process for use in instrumental and reference potential calibration in organic solvent media [3–5]. To this aim both cyclic voltammetry with conventional sized electrodes, and recently, steady-state voltammetry with microelectrodes have been employed for evaluating the kinetic and thermodynamic parameters of the $FeCp_2^{+/0}$ couple. The use of $FeCp_2$ for calibrations implies that the rate of the electron transfer is fast and the electrode process exhibits reversible behavior under calibration conditions. A survey in the literature indicated that the kinetic parameters of the $FeCp_2^{+/0}$ couple in pure high-resistance organic solvents, such as ethanol [6], methanol [7], dichloromethane [8], chloroform [9], dichloroethane, nitromethane, nitrobenzene, benzonitrile, butyronitrile, pyridine, tetrahydrofuran, [10], and ACN [11–14] were extensively investigated. In many of these cases, however, the obtained kinetic data disagree with the concept that the oxidation of $FeCp_2$ being a reversible process. Anyhow, since the distortion due to ohmic polarization and charging current effects is

particularly troublesome in high-resistance organic solvents, even if high concentrations of the supporting electrolytes are used, these discrepancies can be attributed to the ohmic drop effects [15, 16].

In the present work, kinetic and thermodynamic properties of the $FeCp_2^{+/0}$ redox couple on either Pt or G-C electrodes in ACN, ACE, and ACN/ACE binary mixtures containing $TBAPF_6$ as supporting electrolyte were investigated by means of EIS and CV at 294.15 K. The half-wave potentials ($E_{1/2}$), the diffusion coefficients (D), and the heterogeneous electron-transfer rate constants (k_s) were determined. The activation-free energies for the electron transfer process ($\Delta G^{\neq}_{exp}$) were determined and compared with the calculated theoretical values ($\Delta G^{\neq}_{cal}$). The interest was focused on the effect of the solvent composition and thus the solvent properties, on the electrochemical behavior of the $FeCp_2^{+/0}$ redox couple. The aim of this work is to assess whether $FeCp_2$ can be used as a voltammetric standard in ACN/ACE solvent mixtures. An exploration of the literature indicated that, with an exception the articles which concern studies on the oxidation of $FeCp_2$ in aqueous solutions of ethanol [17], *N,N*-dimethylformamide [18], and propylene carbonate [18], electrochemical studies on the $FeCp_2^{+/0}$ couple in binary solvent systems are still very rare, and therefore demand further investigation. Consequently, the present article constitutes the first systematic evaluation of the electrochemical properties of the $FeCp_2^{+/0}$ couple in ACN/ACE binary solvent system.

2 Experimental

2.1 Materials

ACN (Merck, puriss. grade) was distilled over phosphorus pentoxide and then redistilled over potassium carbonate, while ACE (Merck, puriss. grade) was dried over calcium chloride and then distilled. The dried solvents were stored over 0.4 nm molecular sieves. The main purpose was to eliminate any traces of water from the solvent. $FeCp_2$ (Fluka, purum. grade) was recrystallized twice from heptane [19], while $TBAPF_6$ (Fluka, purum. grade) was recrystallized twice from absolute ethanol [20], and then dried under reduced pressure at the room temperature for 12 h.

The ACN/ACE binary mixtures were prepared by mass with an uncertainty of $\pm 1 \times 10^{-4}$ g. The estimated error in the mole fraction was $\pm 5 \times 10^{-4}$. A concentrated solution of $TBAPF_6$ (0.10 mol L^{-1}) in appropriate ACN/ACE solvent mixture was used for the preparation of the dilute solution of $FeCp_2$ ($\sim 4 \times 10^{-4}$ mol L^{-1}). The $FeCp_2$ solution was prepared by mass with an uncertainty of $\pm 1 \times 10^{-4}$ g. The conversion of molality (mol kg^{-1}) to molarity (mol L^{-1}) was done using the measured density values of the solvent mixtures (Table 1).

2.2 Apparatus and procedures

The CVs were recorded using a computer-controlled system Zahner/IM6/6EX. The analysis of the obtained CVs was performed using the software Thales (version 4.15). The effect of the uncompensated resistance was reduced by using the positive feedback technique. Therefore, each CV was recorded several times using an experimental setup in which the uncompensated resistance was gradually compensated. To avoid overcompensation and consequently circuit oscillation, no more than 85% of the uncompensated resistance was compensated. The measurements were carried out using a three-electrode cell configuration. The working electrode was either, Pt wire (geometrical area 0.19 cm^2) or G-C wire (geometrical area 0.24 cm^2), the counter electrode was Pt plate, while the reference electrode was Ag/AgCl (KCl sat.). All potentials were recorded relative to the Ag/AgCl (KCl sat.) reference electrode. The cell used was a three-compartment cell designed to minimize the distances between the electrodes with a total solution volume of $\sim$20 mL. The CVs were recorded in the potential region from 0 to +1.0 V versus Ag/AgCl by applying scan rates (v) ranging from 0.02 to 0.12 V s^{-1}. All measurements were carried out at room temperature, which was 294.15 ($\pm$0.5) K.

The EIS spectra were recorded using the computer-controlled system Zahner/IM6/6EX by applying small ac amplitude (10 mV) in a wide frequency range (from 40 to 50 kHz) at the room temperature ($T = 294.15$ K). All

Table 1 Mole fractions of ACN (x_{ACN}), donor numbers (D_N)[a], densities (ρ)[b], refractive indices (n_D)[c], relative permittivities (ε_r), optical permittivities (ε_o), and absolute viscosities (η)[d] of ACN/ACE binary mixtures at 294.15 K

x_{ACN}	D_N	ρ/g cm^{-3}	n_D	ε_r	ε_o	η/mPa s
0.0000	17.0	0.78866	1.3578	20.7	1.844	0.326
0.2595		0.78772	1.3552	24.6	1.837	0.330
0.5911		0.78458	1.3507	29.7	1.824	0.339
0.8047		0.78144	1.3470	32.9	1.814	0.346
1.0000	14.1	0.77792	1.3430	35.9	1.804	0.353

[a] [39]

[b] The density values were experimentally determined by using pycnometer of a volume of 10 mL. The pycnometer was calibrated with distilled water

[c] The refractive indices at the sodium D-line were measured with a thermostated Abbe refractometer (model A. Krüss) with a built-in light source for the measuring prism

[d] The flow times were measured using an Ubbelohde capillary viscometer. The viscometer was calibrated with distilled water in order to determine the constant of the viscometer (0.009903 mm^2 s^{-2})

measurements were performed on either Pt or G-C working electrodes against the reference electrode Ag/AgCl (KCl sat.) with Pt plate as counter electrode. In all cases the EIS spectra were recorded in a potential which corresponds to $E_{1/2}$ of the $FeCp_2^{+/0}$ redox couple. The EIS spectra were analyzed using the software Thales (version 4.15).

3 Results and discussion

3.1 Cyclic voltammetry

The measured physicochemical properties of the ACN/ACE liquids mixtures such as densities, viscosities, and refractive indices are reported in Table 1. Selective electrochemical data of the $FeCp_2^{+/0}$ couple in ACN, ACE, and ACN/ACE solvent mixtures obtained in the present work on either Pt or G-C working electrodes at the scan rate of $v = 0.10$ V s^{-1} and the temperature of $T = 294.15$ K are presented in Table 2. Representative CVs of $FeCp_2^{+/0}$ in selected ACN/ACE mixtures recorded on either Pt or G-C electrodes at $v = 0.10$ V s^{-1} are presented in Fig. 1.

Table 2 Mole fractions of ACN (x_{ACN}), anodic (E_p^{ox}), and cathodic (E_p^{red}) peak potentials[a], anodic and cathodic peak current ratios (i_p^{ox}/i_p^{red}), peak potential separations (ΔE_p)[b], half-wave potentials ($E_{1/2}$)[ac], and heterogeneous electron-transfer rate constants (k_s) for $FeCp_2$ ($\sim 4 \times 10^{-4}$ mol L^{-1}) in ACN/ACE binary mixtures (0.1 mol L^{-1} $TBAPF_6$) at $v = 0.10$ V s^{-1} and $T = 294.15$ K. The CVs were recorded on either platinum (Pt) (geometrical area 0.19 cm^2)[d] or glassy carbon (G-C) (geometrical area 0.24 cm^2)[d] electrodes

Electrode	E_p^{ox}/V	E_p^{red}/V	i_p^{ox}/i_p^{red}	ΔE_p/V	$E_{1/2}$/V	10^2 k_s/cm s^{-1}
$x_{ACN} = 1.0000$						
G-C	0.464	0.366	1.00	0.098	0.415	0.89
Pt	0.454	0.377	1.01	0.077	0.416	2.57
$x_{ACN} = 0.8047$						
G-C	0.480	0.389	1.00	0.091	0.435	1.26
Pt	0.474	0.397	1.00	0.077	0.436	2.69
$x_{ACN} = 0.5911$						
G-C	0.502	0.409	0.99	0.093	0.456	1.23
Pt	0.494	0.415	1.00	0.079	0.454	2.56
$x_{ACN} = 0.2595$						
G-C	0.515	0.425	1.01	0.090	0.470	1.51
Pt	0.510	0.432	1.03	0.078	0.471	2.84
$x_{ACN} = 0.0000$						
G-C	0.525	0.447	1.02	0.078	0.486	2.74
Pt	0.524	0.446	1.04	0.078	0.485	2.96

[a] The potential values are referenced to the Ag/AgCl (KCl sat.) reference electrode

[b] $\Delta E_p = (E_p^{ox} - E_p^{red})$

[c] $E_{1/2} = (E_p^{ox} + E_p^{red})/2$

[d] The active surface area of the working electrodes was experimentally determined by measuring a solution of $FeCp_2$ (4.0×10^{-4} mol L^{-1}) in ACN (0.1 mol L^{-1} $TBAPF_6$) using the D value of $D = 2.17 \times 10^{-5}$ cm^2 s^{-1} [40]

As it can be observed in Fig. 1, the CVs were found to be symmetric with equal cathodic (i_p^{red}) and anodic (i_p^{ox}) peak currents and consequently the i_p^{ox}/i_p^{red} ratio approaches the unity in all the investigated ACN/ACE mixtures over the whole v range. The results indicate that the oxidized and the reduced forms are always equal and are not consumed in a coupled chemical reaction, confirming, therefore, that the charge-transfer process is either reversible or quasi-reversible. It is interesting, however, to mention that the values of the peak-to-peak separation ($\Delta E_p = E_p^{ox} - E_p^{red}$) obtained for CVs recorded without the compensation of the uncompensated resistance were found to be larger than the theoretical value of 0.06 V (at 298.15 K) and tend to increase with the progressive increase of v. The large ΔE_p values and their variations with v indicate the high degree of distortion arising from the influence of the uncompensated resistance. This observation proves that the uncompensated resistance effect leads to the determination of inaccurately ΔE_p values, and consequently, to incorrect values of heterogeneous rate constant (k_s), given that the determination of k_s is based on the degree of peak separation between the forward and reverse scans. However, during the compensation of the uncompensated resistance, ΔE_p progressively decreases to reach finally within experimental error ΔE_p values in the range 0.068–0.100 V depending on the composition of the ACN/ACE solvent system. Representative CVs recorded for $FeCp_2$ in pure ACN on Pt electrode at $v = 0.12$ V s^{-1} with either the absence or presence of resistance compensation, are presented in Fig. 2. As it can be observed, the shape of the CV slightly changes (ΔE_p decreases) as the uncompensated resistance is compensated. The variation of ΔE_p with the progressive compensation of uncompensated resistance observed for these CVs is shown in the inset of Fig. 2. It can be observed that ΔE_p decreases almost linearly with the addition of resistance.

The half-wave potentials ($E_{1/2}$) of the $FeCp_2^{+/0}$ redox couple in various ACN/ACE solvent mixtures were determined from the anodic (E_p^{ox}) and cathodic (E_p^{red}) peak potentials, assuming that the diffusion coefficients for the oxidized and reduced species are similar, according to the following equation:

$$E_{1/2} = E_p^{ox} - \Delta E_p/2 \quad (1)$$

where ΔE_p is the potential difference between anodic and cathodic peaks ($\Delta E_p = E_p^{ox} - E_p^{red}$). The $E_{1/2}$ values were estimated with experimental error of $\pm 5 \times 10^{-3}$ V. The $E_{1/2}$ values are reported in Table 2 and presented graphically versus the mole fraction of ACN (x_{ACN}) in Fig. 3. The $E_{1/2}$ values were found to be constant within experimental error without depending on v, which is a typical behavior

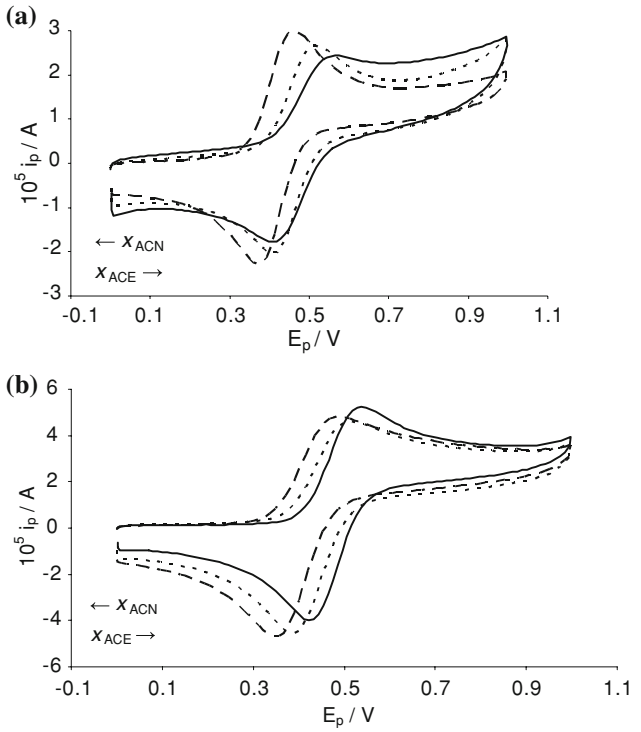

Fig. 1 Representative CVs of $FeCp_2$ ($\sim 4 \times 10^{-4}$ mol L^{-1}) in selected ACN/ACE binary mixtures (0.1000 mol L^{-1} $TBAPF_6$) recorded on either **a** Pt or **b** G-C electrodes at $v = 0.10$ V s^{-1} and $T = 294.15$ K. The CVs correspond to the following ACN/ACE binary mixtures: $x_{ACN} = 0.0000$ (*solid line*), $x_{ACN} = 0.5911$ (*dotted line*), and $x_{ACN} = 1.0000$ (*dashed line*)

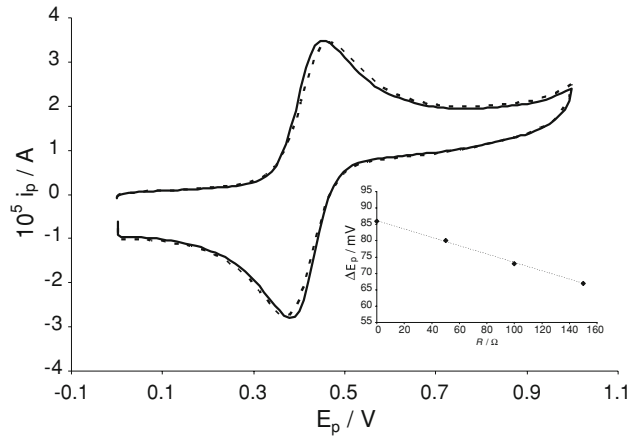

Fig. 2 Representative CVs recorded for $FeCp_2$ ($\sim 4 \times 10^{-4}$ mol L^{-1}) in pure ACN (0.1000 mol L^{-1} $TBAPF_6$) on Pt electrode before and after compensation of the uncompensated resistance at $v = 0.12$ V s^{-1} and $T = 294.15$ K. The CVs are denoted as follows: CV obtained after compensation (*solid line*), CV recorded before compensation (*dotted line*). Inset: Variation of the peak potential separation (ΔE_p) with progressive compensation of uncompensated resistance

for reversible redox couples. It can be observed that the $E_{1/2}$ values shift to less positive potentials with the increase of the content of ACN, demonstrating that the oxidized

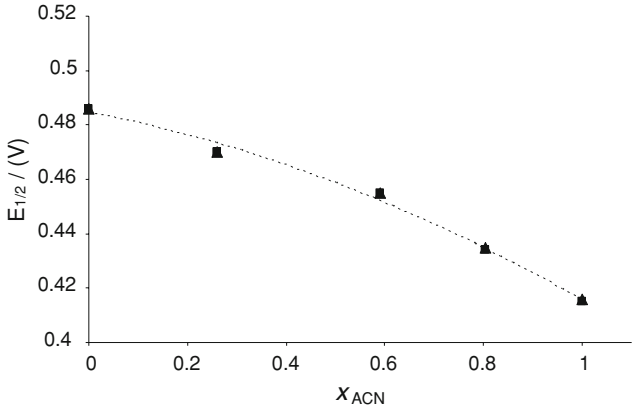

Fig. 3 Variation of the half-wave potential ($E_{1/2}$) with the mole fraction of ACN (x_{ACN}) for the oxidation of $FeCp_2$ ($\sim 4 \times 10^{-4}$ mol L^{-1}) in ACN/ACE binary mixtures (0.1 mol L^{-1} $TBAPF_6$) on either Pt (*filled triangle*) or G-C (*filled square*) electrodes at $T = 294.15$ K

$FeCp_2^+$ species are formed more effortless in ACN while the neutral $FeCp_2$ species have a preference to ACE. It is interesting, however, that the determined $E_{1/2}$ values demonstrate that the position of the formal potential of the $FeCp_2^{+/0}$ redox couple is affected by changing the composition, and thus by varying the physical properties of the mixed solvent medium. This variation of $E_{1/2}$ with the change of the solvent composition can be explained through the differences in physical properties (such as dipole moments, dielectric constants) of the ACN and ACE molecules. It is well known that the electrochemical oxidation of ferrocene corresponds to a reversible change between the neutral reduced form $FeCp_2$ and the oxidized cationic form $FeCp_2^+$. The oxidized $FeCp_2^+$ species are more sensitive to interactions with the polar solvent molecules than the reduced neutral $FeCp_2$ species. Therefore, the strength of the interactions of $FeCp_2^+$ (which acts as Lewis acid) with the solvent molecules (they act as Lewis base) is expected to have an effect on the oxidation process of ferrocene, and consequently on the $E_{1/2}$ value of the $FeCp_2^{+/0}$ couple. Thus, a strong electron contribution of the solvent molecule to $FeCp_2^+$ results to its stabilization and thus in diminution of the $E_{1/2}$ value. It is, therefore, obvious that ACN having larger dipole moment ($\mu = 3.92$ D) [21] and greater dielectric constant ($\varepsilon = 35.9$) compared to ACE ($\mu = 2.88$ D, $\varepsilon = 20.7$) [21] can preferentially stabilize the $FeCp_2^+$ species with a consequence the decrease of $E_{1/2}$ of the $FeCp_2^{+/0}$ redox couple.

The peak current for a reversible or a quasi-reversible process is described by the Randles–Sevcik equation [22, 23] which assumes mass transport only by diffusion process:

$$i_p = 0.4463nF(nF/RT)^{1/2}AD^{1/2}cv^{1/2} \quad (2)$$

where i_p is the peak current, n the number of electrons exchanged during the reversible or quasi-reversible process namely the electron stoichiometry, A the active surface area of the working electrode, D the diffusion coefficient, c the bulk concentration of the diffusing species, v the voltage scan rate, F the Faraday constant, R the gas constant, and T the absolute temperature. The D values of $FeCp_2$ in various ACN/ACE mixtures were determined from Eq. 2 and are reported in Table 3. The results indicate that D decreases non-linearly with the progressive increase of the ACN content. In fact, the experimental D values given in Table 3 can be fitted with second order polynomials with R-squared values equal to unity ($R^2 \approx 1$). The non-linear diminution of D with the enrichment of the mixture in ACN is attributed probably to the corresponding non-linear increase of the viscosity of the solvent medium (Table 1). The last observation can be ascribed to the "non ideal" behavior of the investigated binary mixtures resulted most probable from the strong dipole–dipole interactions between the unlike molecules.

The determined D values were used for the estimation of the hydrodynamic radius of the diffusing species (r_s) in each solvent medium by using the corrected version of the Stokes–Einstein relation [24]:

$$r_s = k_B T / 2\pi\eta D \quad (3)$$

Where k_B is the Boltzmann's constant, T is the absolute temperature, and η is the viscosity of the medium (Table 1). By plotting the measured values of D vs. $1/\eta$ a straight-line plot was obtained. From the slope of the line and the Eq. 3 the r_s value of $r_s = 0.33$ nm was determined which is slightly smaller than the crystallographic radius of $FeCp_2$ (0.365 nm) [25].

The data obtained from CVs were further analyzed for the determination of the heterogeneous electron-transfer rate constant (k_s) of the $FeCp_2^{+/0}$ couple according to the electrochemical absolute rate relation proposed by Nicholson [26, 27], which is based on the degree of peak separation ΔE_p between the forward and the reverse scans:

$$\psi = \gamma^a k_s \Big/ \sqrt{n\pi F v D_o / RT} \quad (4)$$

where ψ is a kinetic parameter, a the charge-transfer coefficient, D_o, D_R the diffusion coefficients of the oxidized and reduced species, respectively, n the number of the electrons involved in the reaction ($n = 1$), and γ a parameter given from the relation: $\gamma = (D_o/D_R)^{1/2}$. The other symbols have their usual meanings. The ψ parameter is related to the experimentally determined values of ΔE_p, and according to Nicholson, large ψ values characterize reversible electron-transfer process, while when $\psi \approx 0$ the electron process can be recognized as totally irreversible. Intermediate ψ values characterize quasi-reversible process. For the present work the values of ψ were calculated from the experimental ΔE_p values according to the reference curve $\Delta E_p = f(\psi)$ which was constructed from data reported in the literature [26] considering that $a = 0.5$. The range of the potential scan rate employed in the present work (0.02−0.12 V s^{-1}) corresponds to a peak separation range of 0.068 V $< \Delta E_p <$ 0.100 V in which the Nicholson analysis is reliable. The determined k_s values of the $FeCp_2^{+/0}$ couple in ACN/ACE mixtures at $v = 0.10$ V s^{-1} are included in Table 2, while the average values of k_s determined in the scan rate range from 0.02 to 0.12 V s^{-1} are summarized in Table 3. The k_s values are presented graphically versus the solvent composition in Fig. 4. As it can be observed in Fig. 4 the rate of electron transfer seems to change with the variation of the solvent composition. In fact, it can be concluded that the electron transfer is in general faster on the Pt electrode compared to that on the G-C electrode. There is also a trend of k_s to increase with the increase of the ACE content. Previous published articles which concerned k_s measurements of the $FeCp_2^{+/0}$ couple on Pt working electrode in either pure ACE or ACN revealed k_s values, which were ranged from 0.017 to 0.22 cm s^{-1} (Table 3). The differences observed between the k_s values can be attributed to the dissimilar sizes of the Pt working electrodes used in each case. It is well known that k_s values measured using ultra

Table 3 Mole fractions of ACN (x_{ACN}), molar concentrations of $FeCp_2$ (c), diffusion coefficients (D), the average values of the heterogeneous electron-transfer rate constant (k_s) for $FeCp_2$ ($\sim 4 \times 10^{-4}$ mol L^{-1}) in ACN/ACE binary mixtures (0.1 mol L^{-1} $TBAPF_6$) at 294.15 K

x_{ACN}	$10^4 \times c$/mol L^{-1}	$10^5 \times D$/ cm^2 s^{-1}		$10^2 \times k_s$/cm s^{-1}	
		G-C	Pt	G-C	Pt
1.0000	3.97	1.40	1.85	1.16	2.31
			2.4[b]/2.4[f]		4.4[a]/9.0[b]
			2.2[h]/2.24[i]		1.7[c]/5.2[e]
			2.07[e]		3.5–7.6[d]/22 ± 4[g]
0.8047	3.89	1.60	2.03	1.22	2.44
0.5911	3.30	1.80	2.23	1.28	2.51
0.2595	3.40	2.10	2.50	1.48	2.66
0.0000	3.20	2.32	2.70	2.08	2.78
			2.76[i]		8.0[b]

[a] [6], ACN (0.1 M TEAP), Pt working electrode

[b] [10], ACN (0.1 M TBAP), Pt working electrode, 295.15 K

[c] [41], ACN (0.1 M $TEABF_4$), Pt working electrode, 293.15 K

[d] [8], ACN (0.1 M TBAP), Pt working electrode, 295.15 K

[e] [42], ACN (0.1 M TBAP), Pt electrode, 298.15 K

[f] [43], ACN (0.2 M $LiClO_4$), Pt electrode, 298.15 K

[g] [44]

[h] [40]

[i] [45] ACN (0.1 M $TBAPF_6$), Pt electrode, 298.15 K

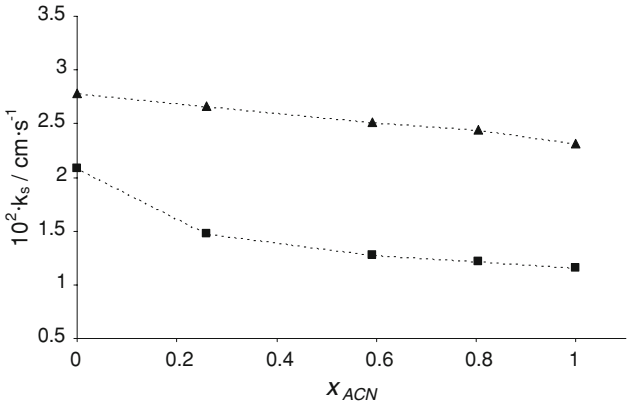

Fig. 4 Variation of the heterogeneous electron-transfer rate constant (k_s) with the mole fraction of ACN (x_{ACN}) for $FeCp_2$ ($\sim 4 \times 10^{-4}$ mol L^{-1}) in ACN/ACE binary mixtures (0.1 mol L^{-1} $TBAPF_6$) on either Pt (*filled triangle*) or G-C (*filled square*) electrodes at $T = 294.15$ K

microelectrodes are clearly greater than those obtained by using conventionally Pt electrodes of normal size. This observation can be ascribed to the increase of passivity of the surface of electrode through a film (or coating) formation, something which occurs on normal-size electrodes but not on microelectrodes [28].

For simple heterogeneous redox reactions between an electrode and electro-active species, which are associated with only slight differences in molecular structure among oxidized and reduced forms (e.g., no bond fracture or formation occurs), the equation of Marcus [29, 30] can be applied in order to calculate the activation free energies for the electron transfer process ($\Delta G^{\neq}_{exp}$) from the obtained k_s values:

$$k_s = \kappa\theta Z_{het} \exp\left(-\Delta G^{\neq}_{exp}/RT\right) \quad (5)$$

where κ is the transmission coefficient and θ is a displacement fluctuation parameter. Z_{het} represents the collision frequency of the reactant molecules upon the electrode surface and it was calculated as $Z_{het} = 4.57 \times 10^3$ cm s^{-1} at $T = 294.15$ K from the relation: $Z_{het} = (k_B T/2\pi m)^{1/2}$, where m is the reduced mass of reactant species, namely of $FeCp_2$ ($m = 3.09 \times 10^{-22}$ g molecule^{-1}). The activation free energy for electron transfer $\Delta G^{\neq}_{exp}$ determined from Eq. 5 includes the solvent repolarization effect, which can be treated theoretically using the Born relation (Eq. 6), and the internal structural reorganization, which can be assessed from bond force constants and changes in bond lengths [31]. Assuming that the oxidation of $FeCp_2$ is adiabatic reaction, and consequently, that both κ and θ parameters are equal to unity, the $\Delta G^{\neq}_{exp}$ values for the $FeCp_2^{+/0}$ redox couple in various ACN/ACE mixtures can be calculated from the Eq. 5. The uncertainty for the determination of $\Delta G^{\neq}_{exp}$ was found to be $\pm 5\%$ and it can be considered acceptable. The $\Delta G^{\neq}_{exp}$ values obtained in various ACN/ACE mixtures are reported in Table 4.

A comparison between the experimental ($\Delta G^{\neq}_{exp}$) and the theoretical ($\Delta G^{\neq}_{cal}$) activation free energy values was considered to be essential in order to get information concerning the degree of the contribution of the internal structural reorganization effect on $\Delta G^{\neq}_{exp}$. The theoretical $\Delta G^{\neq}_{cal}$ values were calculated according to the equation proposed by Born, which is valid for changes in a dielectric continuum, and includes only the solvent repolarization effect:

$$\Delta G^{\neq}_{cal} = \left(e^2/8r\right)\left[1/\varepsilon_o - 1/\varepsilon_r\right] \quad (6)$$

where r is the crystallographic radius of the reactant molecule, namely of the $FeCp_2$ molecule ($r = 0.365$ nm), ε_o and ε_r are the values of optical and relative permittivity of the solvent medium, respectively, and e is the electronic charge. The ε_o values for the various ACN/ACE mixtures were calculated from the experimental values of the refractive index (n_D) (Table 1) using the well-known relation: $n_D = (\varepsilon_o)^{1/2}$. The values of ε_r were calculated from a reference curve which was constructed using the values of $\varepsilon_r = 35.9$ (298.15 K) [32] for ACN and $\varepsilon_r = 20.7$ (298.15) for ACE [33], assuming that the ACN/ACE binary system behaves almost as an ideal mixture. The determined $\Delta G^{\neq}_{cal}$ values are included in Table 4. As it can be observed the disagreement between the theoretical $\Delta G^{\neq}_{cal}$ and the experimental $\Delta G^{\neq}_{exp}$ values seems to be relatively small ($\sim 10\%$). However, considering that the error for determining $\Delta G^{\neq}_{exp}$ is about $\sim 5\%$, the results indicate that the contribution of the internal structural reorganization effect to the overall activation energy is not considerably significant. Consequently,

Table 4 Mole fractions of ACN (x_{ACN}), and activation Gibbs energies for electron transfer ($\Delta G^{\neq}$) for $FeCp_2$ ($\sim 4 \times 10^{-4}$ mol L^{-1}) in ACN/ACE binary mixtures (0.1 mol L^{-1} $TBAPF_6$) at 294.15 K

x_{ACN}	$\Delta G^{\neq}_{exp}$/eV molecule^{-1} [a]		$\Delta G^{\neq}_{cal}$/eV molecule^{-1} [b]
	G-C	Pt	
1.0000	0.33	0.31	0.26
		0.30 ± 0.01[c]	0.26[c]
		0.26[d]	0.26[d]
0.8047	0.33	0.31	0.26
0.5911	0.32	0.31	0.25
0.2595	0.32	0.31	0.25
0.0000	0.31	0.30	0.24

[a] Experimental $\Delta G^{\neq}$ values calculated from the Marcus relation, Eq. 5

[b] Theoretical $\Delta G^{\neq}$ values calculated from the Born relation, Eq. 6

[c] [41] at 293.15 K

[d] [44] at 298.15 K

it is obvious that the Fe^{3+}/Fe^{2+} redox pair in the $FeCp_2$ molecule is well shielded from its environment, namely the Cp rings, and therefore, the differences in bond lengths in charged and non-charged species are small [34]. According to previous reports [35], the contribution of the internal structural reorganization effect to the total $\Delta G^{\neq}$ for systems, in which delocalization of the acquired charge occurs, is less than approximately 5%. The results of the present work seem to be in accordance with these reports.

3.2 Electrochemical impedance spectroscopy

Representative EIS spectra (Nyquist plots) of the imaginary part of impedance (Z_{im}) versus the real part of impedance (Z_{re}) for $FeCp_2$ in pure ACN ($x_{ACN} = 1.0000$) recorded at the CV-peak potential of the electron transfer step (at 0.415 V versus Ag/AgCl) on either Pt or G-C in the frequency range from 40 to 50 kHz, are shown in Fig. 5. The Nyquist plots yield a straight line with an angle of nearly 45° with the Z_{re} axis at sufficiently low frequencies, with a partially resolved semicircle at high frequencies. The EIS results demonstrate that the diffusion of $FeCp_2$ species in the solution is the rate-determining step in the whole process, and consequently, the process can be characterized as diffusion-controlled process. This behavior reveals also that the k_s values of the $FeCp_2^{+/0}$ redox couple must be greater than $k_s > 0.01$ cm s^{-1} [36, 37]. These results are in accordance with the CV results (Table 3). Furthermore, it has been observed that the impedance behavior revealed the expected dependence on dielectric constant of the bulk solvent medium. As an example the EIS spectra recorded for $FeCp_2$ on G-C electrode in three different ACN/ACE binary mixtures in the frequency range from 40 to 50 kHz are shown in Fig. 6. It is obvious that the bulk resistance, and thus the impedance, enhance with the enrichment of the

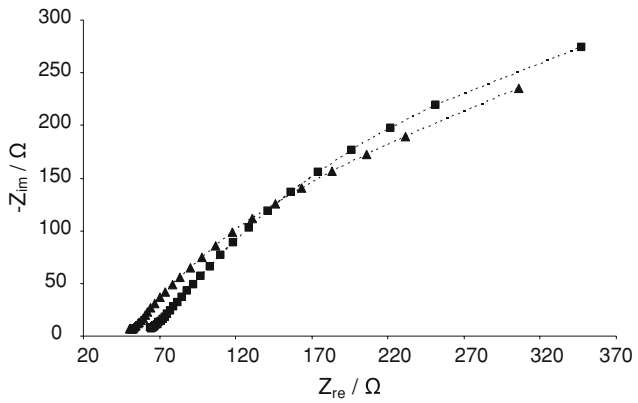

Fig. 5 EIS Spectra of $FeCp_2$ ($\sim 4 \times 10^{-4}$ mol L^{-1}) in pure ACN (0.1 mol L^{-1} $TBAPF_6$) recorded at 0.415 V versus Ag/AgCl on either Pt (*filled triangle*) or G-C (*filled square*) in the frequency range from 40 to 50 kHz

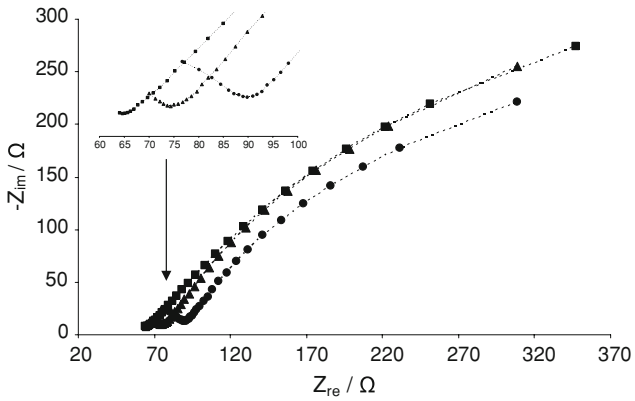

Fig. 6 EIS Spectra of $FeCp_2$ ($\sim 4 \times 10^{-4}$ mol L^{-1}) in various ACN/ACE binary mixtures (0.1 mol L^{-1} $TBAPF_6$) recorded on G-C electrode in the frequency range from 40 to 50 kHz. The EIS spectra correspond to the following ACN/ACE binary mixtures: $x_{ACN} = 1.0000$ (*filled square*), $x_{ACN} = 0.5911$ (*filled triangle*), and $x_{ACN} = 0.0000$ (*filled circle*)

binary mixture in ACE, as a consequence of the decrease of the dielectric constant of the solvent medium (Table 1) [38]. The EIS results were analyzed by fitting various electrical equivalent circuit models in order to obtain the "best" fitting circuit model which represents the investigated system. A very good agreement between the experimental and simulated impedance results was obtained using the electrical equivalent circuit ($R_1 + (R_2/C_3 + (R_4/C_5))$) (inset of Fig. 7). The electrochemical parameters of the ($R_1 + (R_2/C_3 + (R_4/C_5))$) equivalent circuit, which represents the electrode/$FeCp_2$/electrolyte configuration, were

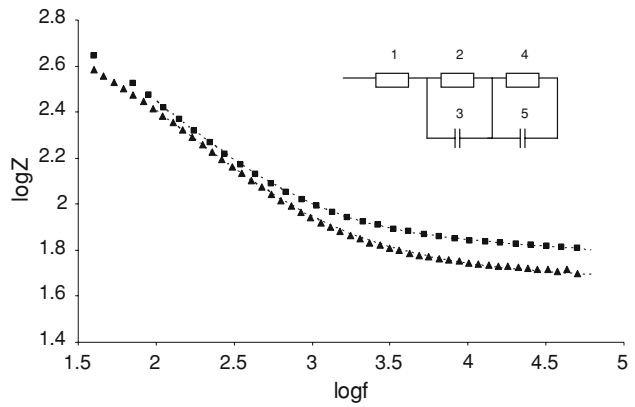

Fig. 7 Bode plots for $FeCp_2$ ($\sim 4 \times 10^{-4}$ mol L^{-1}) in pure ACN (0.1 mol L^{-1} $TBAPF_6$) recorded on either Pt (*filled triangle*) or G-C (*filled square*) electrodes in the frequency (*f*) range from 40 to 50 kHz. The points represent the experimental values of impedance while the *dotted lines* represent the corresponding simulated values (determined by using the software Thales, version 4.15). Inset: The electrical equivalent circuit ($R_1 + (R_2/C_3 + (R_4/C_5))$) which represents the investigated system electrode/$FeCp_2$/electrolyte. The numbers 1, 2, and 4 represent the resistors R_1, R_2, and R_4, respectively, while the numbers 3 and 5 represent the capacitors C_3 and C_5, respectively (Table 5)

Table 5 EIS parameters, such as resistances (R) and capacitances (C) of the circuit shown in Fig. 10 which corresponds to the investigated system $FeCp_2$ ($\sim 1 \times 10^{-4}$ mol L^{-1}) in ACN/ACE binary mixtures (0.10 mol L^{-1} NBu_4PF_6) on either Pt or G-C electrodes

Element	x_{ACN}[a]				
	0.0000	0.2595	0.5911	0.8047	1.0000
G-C					
R_1/Ω	39.75	25.80	36.23	38.05	50.63
R_2/Ω	48.52	57.64	38.59	60.46	19.25
C_3/nF	46.48	111.5	61.53	72.25	1034
$R_4/k\Omega$	0.753	3.158	0.949	2.955	0.994
$C_5/\mu F$	4.305	3.33	4.026	2.262	3.231
Pt					
R_1/Ω	41.29	24.64	43.41	31.09	39.41
R_2/Ω	51.65	64.53	71.58	46.11	13.20
C_3/nF	109.4	142.4	26.21	64.35	1218
$R_4/k\Omega$	298.9	1.544	1.442	1.039	0.837
$C_5/\mu F$	2.344	3.146	3.303	2.941	3.12

[a] Mole fractions of ACN

determined by employing the software Thales (version 4.15) and are reported in Table 5. As an example, representative Bode diagrams obtained for both electrodes in pure ACN are shown in Fig. 7. As it can be observed in Fig. 7 the experimental and the simulated impedance values are in absolute agreement indicating that the equivalent circuit $(R_1 + (R_2/C_3 + (R_4/C_5)))$ represents the experimental data obtained for the system electrode/$FeCp_2$/electrolyte.

4 Conclusions

In the present work the $FeCp_2^{+/0}$ redox couple was investigated by means of CV and EIS in ACN, ACE, and ACN/ACE binary mixtures on either Pt or G-C working electrodes at 294.15 K. The electron-transfer process was found to be reversible and diffusion-controlled in all investigated ACN/ACE binary mixtures, and thus the $FeCp_2^{+/0}$ couple can be used as a standard reference couple in such solvent system. The results indicated a shift of the $E_{1/2}$ values to less positive potentials with the increase of the ACN content, while the working electrode material had a negligible effect on $E_{1/2}$. A slight variation of k_s with the composition of the mixed solvent was observed, namely the k_s was increased with the enrichment of the binary mixture in ACE. Contributions to $\Delta G^{\neq}_{exp}$ arising from changes in the internal coordinates of $FeCp_2$ upon the electron transfer process were found to be negligible. The EIS data confirmed that the diffusion of the $FeCp_2$ species in the solution is the rate-determining step and consequently that the process can be characterized as diffusion-controlled. The analysis of the EIS data demonstrated that the electrical equivalent circuit $(R_1 + (R_2/C_3 + (R_4/C_5)))$ represents the investigated system electrode/$FeCp_2$/electrolyte.

Acknowledgments The authors would like to thank Mrs. D. Schneider (TU Ilmenau).

References

1. Seibold EA, Sutton LE (1955) J Chem Phys 23:1967
2. Geiger WE (1990) Organometallic radical processes. Elsevier, Amsterdam (and references therein)
3. Zhu T, Su CH, Lemke BK, Wilson LJ, Kadish KM (1983) Inorg Chem 22:2527
4. Kadish KM, Su CH (1983) J Am Chem Soc 105:177
5. Gritzner G, Kuta J (1982) J Pure Appl Chem 54:1527
6. Diggle JW, Parker AJ (1973) Electrochim Acta 18:975
7. Saji T, Maruyama Y, Aoyagvi S (1978) J Electroanal Chem 86:219
8. Bond AM, Henderson TLE, Mann DR, Mann TF, Thormann W, Zoski CG (1988) Anal Chem 60:1878
9. Pournaghi-Azar MH, Ojani R (1994) Electrochim Acta 39:953
10. Kadish KM, Ding JQ, Malinski T (1984) Anal Chem 56:1741
11. Kamau GN, Saccucci TM, Gounilli G, Nassar AEF, Rusling JF (1994) Anal Chem 66:994
12. Daschbach J, Blackwood D, Pons JW, Pons S (1987) J Electroanal Chem 237:269
13. Crooks RM, Bard AJ (1988) J Electroanal Chem 243:117
14. Bond AM, Oldham KB, Snook GA (2000) Anal Chem 72:3492
15. Wightman RM (1981) Anal Chem 53:1125
16. Howell JO, Wightman RM (1984) Anal Chem 56:524
17. Daniele S, Baldo MA, Bragato C (1999) Electrochem Commun 1:37
18. Zara AJ, Machado SS, Bulhoes LOS, Benedetti AV, Rabockai T (1987) J Electroanal Chem 221:165
19. Quirk PF, Kratochvil B (1970) Anal Chem 42:535
20. Hartl F, Mahabiersing T, Le Floch P, Mathey F, Ricard L, Rosa P, Záliš S (2003) Inorg Chem 42:4442
21. CRC (2003/2004) Handbook of chemistry and physics, 84th ed. CRC Press, Boca Raton, FL
22. Randles JEB (1948) Trans Faraday Soc 44:327
23. Comminges C, Barhdadi R, Laurent M, Troupel M (2006) J Chem Eng Data 51:680
24. Wasserscheid P, Keim W (2000) Angew Chem Int Ed 39:3772
25. Fischer DW (1964) Acta Cryst 17:619
26. Nicholson RS (1965) Anal Chem 37:1351
27. Kanatharana P, Spritzer MS (1974) Anal Chem 46:958
28. Bond AM, Henderson TLE, Thorman WJ (1986) J Phys Chem 90:2911
29. Marcus RA (1965) J Chem Phys 43:679
30. Marcus RA (1968) Electrochim Acta 13:995
31. Bockris JOM, Khan SUM (1979) Quantum electrochemistry. Plenum Press, New York
32. Goldfarb DL, Longinotti MP, Corti HR (2001) J Solution Chem 30:307
33. Reynolds BB, Kraus CA (1948) J Am Chem Soc 70:1709
34. Bernstein T, Herbstein FH (1968) Acta Cryst B24:1640
35. Halle JM (1971) Reactions of molecules at electrodes. Wiley, London
36. Mohran HS (2005) Am J Appl Sci 2:1629
37. Rashwan F (2005) Am J Appl Sci 2:1595
38. Kim DJ, Ryu HS, Kim IP, Cho KK, Nam TH, Kim KW, Ahn JH, Ahn HJ (2007) Phys Scr T129:70

39. Marcus Y (1984) J Solution Chem 13:599
40. Baur JE, Wightman RM (1991) J Electroanal Chem 305:73
41. Sharp M (1983) Electrochim Acta 28:301
42. Moharram YI (2006) J Electroanal Chem 587:115
43. Kuwana T, Bublitz DE, Hoh G (1960) J Am Chem Soc 82:5811
44. Sharp M, Peterson M, Edström K (1980) J Electroanal Chem 109:271
45. Tsierkezos NG (2007) J Solution Chem 36:289